Journal of Power Sources 235 (2013) 117–121

Contents lists available at SciVerse ScienceDirect

Journal of Power Sources

journal homepage: www.elsevier.com/locate/jpowsour

Short communication

Water-stable lithium anode with $Li_{1.4}Al_{0.4}Ge_{1.6}(PO_4)_3$–$TiO_2$ sheet prepared by tape casting method for lithium-air batteries

Ming Zhang [a,b], Keita Takahashi [b], Ichiro Uechi [b], Yasuo Takeda [b], Osamu Yamamoto [b,*], Dongmin Im [c], Dong-Jonne Lee [c], Bo Chi [a], Jian Pu [a], Jian Li [a], Nobuyuki Imanishi [b]

[a] School of Materials Science and Engineering, State Key Laboratory of Material Processing and Die & Mould Technology, Huazhong University of Science and Technology, Wuhan, Hubei 430074, PR China
[b] Department of Chemistry, Faculty of Engineering, Mie University, Tsu, Mie 514-8507, Japan
[c] Samsung Advanced Institute of Technology, Samsung Electronics, Yongin, Gyeonggi 446-712, Republic of Korea

HIGHLIGHTS

- $Li_{1.4}Al_{0.4}Ge_{1.6}(PO_4)_3$ (LAGP)–5 wt.% TiO_2 lithium ion-conducting solid electrolyte sheets were prepared by a tape casting method.
- The composite sheet of LAGP and epoxy resin (about 4 wt.%) was water impermeable.
- The electrical conductivity of the composite sheet was 4.19×10^{-4} S cm^{-1} at 25 °C.
- The Li/$PEO_{18}(CF_3SO_2)_2N$/composite sheet was successfully operated as a lithium electrode in a saturated LiCl aqueous solution.

ARTICLE INFO

Article history:
Received 23 December 2012
Received in revised form
28 January 2013
Accepted 30 January 2013
Available online 13 February 2013

Keywords:
Lithium-air battery
Lithium anode
Lithium ion conductor
NASICON-type 1

ABSTRACT

A $Li_{1.4}Al_{0.4}Ge_{1.6}(PO_4)_3$ (LAGP) sheet was prepared using a tape casting method with a fine LAGP power prepared from a sol–gel precursor. The addition of nanosize TiO_2 as a sintering additive was effective to enhance the ionic conductivity of the tape-cast sheet. The highest electrical conductivity of 8.37×10^{-4} S cm^{-1} was observed for the tape-cast LAGP sheet with 5 wt.% TiO_2 at 25 °C. A hybrid sheet of the tape-cast LAGP and epoxy resin was water impermeable. The electrical conductivity of the water impermeable hybrid sheet with ca. 4% epoxy resin was 4.19×10^{-4} S cm^{-1} at 25 °C. The three-point bending strength of the LAGP–5 wt.% TiO_2–epoxy resin hybrid sheet was 111 N mm^{-2}, which is comparable with a $Li_{1+x+y}Al_xTi_{2-x}P_{3-y}Si_yO$ glass ceramic plate. The Li/$PEO_{18}(CF_3SO_2)_2N$/LAGP–5 wt.% TiO_2–epoxy sheet was successfully operated as a lithium electrode in saturated LiCl aqueous solution.

1. Introduction

Lithium-air rechargeable batteries have theoretically higher energy density than lithium ion batteries, and are therefore attracting increased attention as possible power sources for electric vehicles [1–4]. Two types of lithium-air batteries have been developed; aqueous and non-aqueous systems. The non-aqueous system consists of a lithium electrode, a non-aqueous electrolyte, and an air electrode, and are based on two possible reactions [5]:

$$2Li + O_2 = Li_2O_2, \quad (1)$$

and

$$4Li + O_2 = 2Li_2O. \quad (2)$$

Reaction (1) is reversible, but reaction (2) is irreversible. In the aqueous system, the lithium electrode is protected by a water-stable lithium ion-conducting solid electrolyte, and the cell reaction is [6]:

$$4Li + 6H_2O + O_2 = 4(LiOH \cdot H_2O), \quad (3)$$

where water in the electrolyte is involved in the cell reaction. The calculated energy densities including oxygen are 3460 Wh kg^{-1} for reaction (1) using an open circuit voltage (OCV) of 2.96 V, and 1910 Wh kg^{-1} for reaction (3) using an OCV of 3.0 V. The non-aqueous system has higher energy density than the aqueous

* Corresponding author. Tel.: +81 59 231 9420.
E-mail addresses: osyamamo@alles.or.jp, yamamoto@chem.mie-u.ac.jp (O. Yamamoto).

0378-7753/$ – see front matter © 2013 Elsevier B.V. All rights reserved.
http://dx.doi.org/10.1016/j.jpowsour.2013.01.167

system, but it has some serious problems, including high polarization for the charge and discharge processes, electrolyte decomposition, and contamination by moisture in the air. These problems could be overcome for the aqueous system. The most important issue for the aqueous system is to develop a water-stable lithium electrode, because lithium reacts severely with water and should be covered with a water-stable lithium conducting solid electrolyte. Recently, Visco et al. [7] proposed a water-stable lithium metal electrode protected by an NASCION-type water-stable lithium ion-conducting glass ceramic of $Li_{1+x+y}Al_xTi_{2-x}P_{4-y}Si_yO_{12}$. (LATP). The discharge product of the aqueous lithium-air system is LiOH, and the LiOH is saturated to approximately 5% discharge depth, because of the solubility limit of LiOH in water at room temperature is ca. 5 mol L^{-1}. LATP is unstable in concentrated LiOH aqueous solution, but Imanishi et al. found that LATP is stable in an aqueous solution saturated with LiOH and LiCl [8]. Therefore, LATP could be used as the protective layer of a lithium metal electrode for lithium-air batteries with a LiCl saturated aqueous solution. The LATP glass ceramic, which is supplied by Ohara Co., Japan, had a high lithium ion conductivity of 3.5×10^{-4} S cm^{-1} at room temperature. The glass ceramic was prepared by quenching from the melt and crystallized at high temperature. This glass ceramic is expensive and the sizes are limited. We have previously reported that $Li_{1.4}Al_{0.4}Ge_{1.6}(PO_4)_3$ (LAGP) is stable in an aqueous solution saturated with LiOH and LiCl, and the electrical conductivity is higher than that of $Li_{1.4}Al_{0.4}Ti_{1.6}(PO_4)_3$ [9]. LAGP is the other candidate for the protective layer of the water-stable lithium metal electrode. In this study, we have prepared LAGP thin sheet by the tape casting method, which is suitable for the production of large sized thin sheets. The electrical conductivity, mechanical properties, and water permeability of a hybrid sheet prepared with epoxy resin and the tape-cast sheets were examined. In addition, the stability and charge–discharge performance of the Li/$PEO_{18}Li(CF_3SO_2)_2N$–10% $BaTiO_3$/LAGP–epoxy hybrid sheet/saturated LiCl aqueous solution/Pt cell were examined. LAGP is unstable in contact with lithium metal; therefore, the polyethylene oxide (PEO)-based polymer electrolyte was used as an interlayer between Li and LAGP.

2. Experimental

The NASICON-type LAGP powder was prepared using a precursor prepared by the sol–gel method with citric acid, as reported previously [9]. Stoichiometric amounts of $Ge(OC_2H_5)_4$ (Aldrich), chemical grade $LiNO_3$, $Al(NO_3)_3 \cdot 9H_2O$, and $NH_4H_2PO_4$ were dissolved in a 0.2 M aqueous solution of citric acid and stirred continuously with a magnetic stirrer to obtain a homogeneous solution. A certain volume of ethylene glycol [citric acid:ethylene glycol molar ratio = 1:1, (citric acid + ethylene glycol):($Li^+ + Al^{3+} + Ge^{4+}$) molar ratio = 4:1] was added to the mixed solution to prevent the formation of hard agglomerates and promote polyesterification and polycondensation. The mixed solution was kept at 80 °C during the sol–gel preparation process. After a homogeneous solution was formed, the gel was kept at 170 °C for 1 day to allow the evaporation of water and to promote esterification and polymerization, and the gel was then heated at 500 °C for 4 h. The powder obtained was uniformly ground to a fine powder with an agate mortar and pestle before sintering at 800 °C for 5 h to complete the chemical reaction.

Stoichiometric amounts of LAGP powder made by sol–gel method, and TiO_2 (Aldrich), GeO_2 (Aldrich), or ZrO_2 (Tosoh) fine powers were dispersed in ethanol and toluene mixed solution (3:7 volume ratio) using Menhaden fish oil (2 wt.% to LAGP) as a dispersant. The mixed slurry was then ball milled with ZrO_2 balls for 24 h using high energy mechanical milling (HEMM; Fritsch Planetary Micro Mill). A certain amount of poly(vinyl butyral) (Aldrich, Butvar B-98, 7 wt.% to LAGP) as a binder and butyl benzyl phthalate (7 wt.% to LAGP) as a plasticizer were then added into the mixed slurry and ball milled using HEMM for another 24 h. The slurry was defoamed for 3 min using a planetary vacuum mixer (Thinky, Japan) before casting to remove air bubbles. Tape casting was performed on a silicon coated polyethylene substrate foil using double blades with gap heights of 700 and 400 μm. The casting speed was constant at 60 cm min^{-1}. After tape casting, the green sheets were left to dry at room temperature for 24 h. The green sheet was cut into small pieces of 1.2–1.5 cm × 1.2–1.5 cm. Three green sheets were hot pressed together at 90 °C for 10 min and then sintered at 900 °C in air.

The LAGP and epoxy resin hybrid sheets were prepared by dropping a mixed dilute solution of 1,3-phenylenediamine (1 mol L^{-1}) and 2,2-bis(4-glycidyloxyphenyl)propane (2 mol L^{-1}) in tetrahydrofuran on the surface of LAGP sheet. The LAGP sheets with the epoxy resin solution were kept in vacuum for several minutes to allow the solution to penetrate into the pores of the LAGP sheets. The hybrid sheets were then placed into an oven at 80 °C for 2 h and then at 150 °C for 24 h to allow evaporation of the solvent and to promote polymerization.

The crystal structure of the samples was analyzed using X-ray diffraction (Rigaku RINT-2500) with Cu Kα radiation in the 2θ range from 10 to 90° at a scanning step rate of 0.02° s^{-1}. Impedance measurements of the LAGP–epoxy resin hybrid sheet with gold electrodes sputtered on both surfaces were conducted using an impedance analyzer (Solartron 1260) in the temperature range from 20 to 80 °C and in the frequency range of 0.01 Hz–1 MHz. The impedance profiles were analyzed using a nonlinear instant fit program in the Z-View software. The hybrid sheets were immersed in an aqueous solution with saturated LiOH and LiCl at 60 °C for one week to test their stability. The LAGP sheets were then washed with distilled water and dried in a vacuum oven at 110 °C for 5 h before measuring the electrical conductivity and XRD patterns. The epoxy resin content in the samples was estimated from the weight loss measured by thermogravimetric analysis (TGA; Rigaku Thermoplus TG8120). The three-point bending strength of the LAGP sheet was measured using Shimadzu EZ-S 500 N at room temperature.

The water permeation test was performed using an H-type cell with saturated LiCl aqueous solution on one side and distilled water on the other. The LAGP sheet was packed using a plastic film. The package was then evacuated and heat-sealed apart from a hole with a 6 mm diameter on the LAGP sheet. The water permeation speed through the LAGP sheet was estimated from the change of the chloride ion content in the distilled water over time, measured using a chorine meter (Kasahara Chemical Instruments).

The lithium ion-conducting polymer membrane of PEO_{18}-$Li(CF_3SO_2)_2N$ (LiTFSI)–10% $BaTiO_3$ was prepared using a previously reported casting technique [10]. A certain amount of PEO (Aldrich, average molecular weight 6×10^5) powder and lithium salt of LiTFSI (Aldrich) with Li/O = 1/18 were dissolved in a certain volume of acetonitrile. 10 wt.% nanosize $BaTiO_3$ particles of (100 nm particle size, Sakai Chemical Industry) were added to the solution as the filler. The solution was stirred at room temperature for 24 h in an Ar-filled dry glove box. The homogeneous slurry was then cast into a clean Teflon dish. The acetonitrile solvent was allowed to evaporate slowly in an Ar-filled dry glove box for 24 h, and then dried at 110 °C for 24 h under vacuum. The water-stable lithium anode was assembled by laminating lithium metal, PEO_{18}LiTFSI–10 wt.% $BaTiO_3$ and the LAGP–epoxy resin hybrid sheets in a plastic package, leaving a circular window of 6 mm in diameter. Nickel foil was used as the anodic current collector. The stability and electrochemical performance of the water-stable lithium electrode were examined using a beaker-type cell of Li/PEO_{18}LiTFSI–10 wt.% $BaTiO_3$/LAGP–epoxy/LiCl saturated aqueous solution/Pt, air at 60 °C.

3. Results and discussion

The tape-cast films sintered at 900 °C for 12 h showed single phase NASICON-type LAGP without impurity phases such as $AlPO_4$ and GeO_2. However, the mechanical properties of the tape-cast film were somewhat poor and the relative density was less than 88%. To improve the mechanical properties, fine powders of TiO_2, ZrO_2, and GeO_2 were added into the starting slurry as sintering additives. Fig. 1 shows XRD patterns of the tape-cast LAGP sheets with 5 wt.% TiO_2, 3 wt.% ZrO_2 and 3 wt.% GeO_2, along with the lattice constants. LAGP with 5 wt.% TiO_2 had no diffraction peaks of TiO_2 and the other starting materials. The *c*-lattice parameter of LAGP (2.0625 nm) was decreased (2.0444 nm) and the *a*-lattice parameter remained unchanged by addition of 5 wt.% TiO_2. Some Ti^{4+} cations may substitute for Ge^{4+}. The LAGP sheet with 3 wt.% GeO_2 shows diffraction peaks of GeO_2, and that with 3 wt.% ZrO_2 had peaks indicating $Li_2Zr(PO_4)_3$. The *c*-axis parameter of LAGP with 3 wt.% GeO_2 was 2.0471 nm and the *a*-axis parameter remained unchanged by the addition of GeO_2. The LAGP with 3 wt.% ZrO_2 showed no significant change in either of the *a*- and *c*-lattice parameters.

Fig. 2 shows typical impedance profiles for tape-cast LAGP–5 wt.% TiO_2, LAGP–3 wt.% ZrO_2, and LAGP–3 wt.% GeO_2 at 25 °C, of which the relative densities were 92, 91, and 92%, respectively. These relative densities are slightly higher than that of a sintered pellet of LAGP (89.3%) [9]. The impedance profiles are typical of solid ionic conductors with a blocking electrode [11], which consists of two semicircles, followed by a straight line. The semicircles are attributed to the bulk and grain boundary resistances; however, the semicircle for the bulk resistance was outside the frequency window examined for the samples. The intercept of the semicircle on the real axis at high frequency represents the bulk resistance (R_b), and the diameter of the semicircle is attributed to the grain boundary resistance (R_{gb}). The highest conductivity was observed for LAGP–5 wt.% TiO_2, of which the bulk and grain boundary conductivities at 25 °C were estimated to be 9.54×10^{-4} and 6.83×10^{-3} S cm^{-1}, respectively. The total conductivity was 8.37×10^{-4} S cm^{-1}, which is slightly lower than that of a sintered pellet of LAGP (1.22×10^{-3} S cm^{-1}) [9]. The bulk conductivities of LAGP–3 wt.% GeO_2 and LAGP–3 wt.% ZrO_2 were lower than that of LAGP–5 wt.% TiO_2. A high grain boundary conductivity of 1.21×10^{-2} S cm^{-1} for LAGP–3 wt.% GeO_2 and a low grain boundary

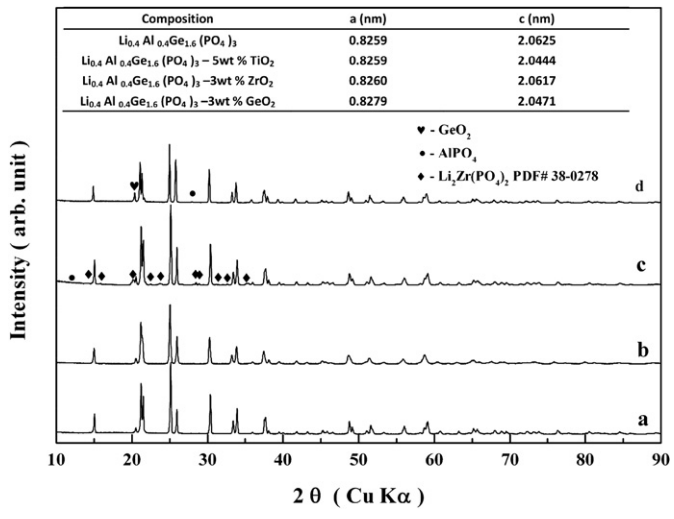

Fig. 1. XRD patterns and lattices parameters of tape-cast (a) LAGP, (b) LAGP–5 wt.% TiO_2, (c) LAGP–3 wt.% ZrO_2, and (d) LAGP–3 wt.% GeO_2.

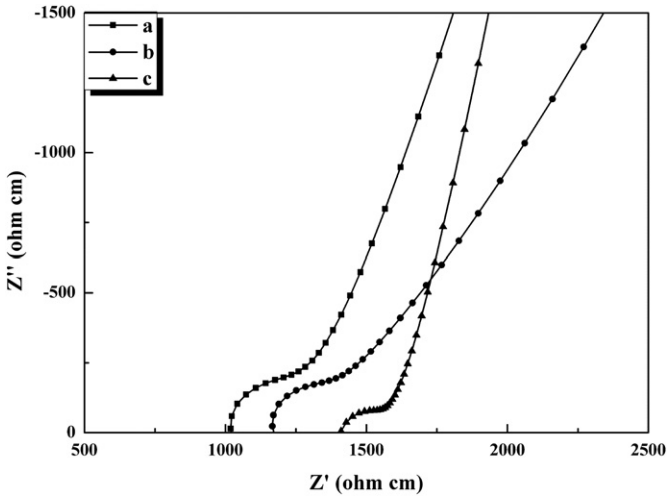

Fig. 2. Impedance profiles of tape-cast LAGP sheets annealed at 900 °C for 12 h at 25 °C; (■) LAGP–5 wt.% TiO_2, (●) LAGP–3 wt.% ZrO_2, and (▲) LAGP–3 wt.% GeO_2.

conductivity of 3.42×10^{-3} S cm^{-1} for LAGP–3 wt.% ZrO_2 were observed. Fig. 3 shows the electrical conductivity at 25 °C of tape-cast sheets of LAGP with TiO_2, ZrO_2, and GeO_2 as a function of the additive content. The highest conductivity was observed for LAGP with 5 wt.% TiO_2. The relative densities of the LAGP–TiO_2 sheets were 88% for LAGP, 87% for LAGP–1 wt.% TiO_2, 89% for LAGP–3 wt.% TiO_2, 92% for LAGP–5 wt.% TiO_2, and 90% for LAGP–7 wt.% TiO_2. The highest conductivity of the LAGP–TiO_2 system was observed for the sample with the highest relative density. The mechanical properties were enhanced by the addition of TiO_2 into LAGP. The three-point bending strength of LAGP at room temperature was 48 N mm^{-2}, which was increased to 74 N mm^{-2} by the addition of 5 wt.% TiO_2. The highest conductivities were observed at 3 wt.% ZrO_2 for LAGP–ZrO_2 and at 3 wt.% GeO_2 for LAGP–GeO_2. The activation energies for electrical conduction were estimated from Arrhenius plots to be 30.1 kJ mol^{-1} for LAGP–5 wt.% TiO_2, 30.2 kJ mol^{-1} for LAGP–3 wt.% ZrO_2, and 30.9 kJ mol^{-1} for LAGP–3 wt.% GeO_2, which are comparable to that of a sintered LAGP pellet at 31.1 kJ mol^{-1} [9].

The important requirement for the protective layer of the water-stable lithium electrode is to minimize water permeation through the sheet. Water permeation tests were conducted using the high conductivity LAGP–5 wt.% TiO_2 sheet sintered at 900 °C for 12 h. Fig. 4 shows the chloride ion transport rate through the film at room temperature, where the thickness of the film was approximately 0.2 mm with a cross-section 0.28 cm^2. A linear increase of the chloride ion concentration over time was observed for the tape-cast LAGP–5 wt.% TiO_2 sheet; therefore, water easily penetrates through this sheet. The water penetration through the sheet may be due to the presence of open pores in the sheet. A dense sintered body could generally be obtained by sintering at a higher sintering temperature for a long sintering period; however, the tape-cast LAGP sheets sintered at 950 °C for 5 h and at 900 °C for 17 h had lower conductivity than that of the tape-cast LAGP sheet sintered at 900 °C for 12 h, due to the evaporation of lithium oxide at high temperature for long sintering periods. To suppress water permeation through the LAGP sheet, the open pores were filled with epoxy resin, which is stable in water, as reported in our previous paper [12]. The water permeation test results through the LAGP–5 wt.% TiO_2–epoxy resin hybrid sheet are shown in Fig. 4. TGA suggested that the content of epoxy resin in the hybrid sheet was ca. 4 wt.%. No chloride ions were detected in the distilled water side

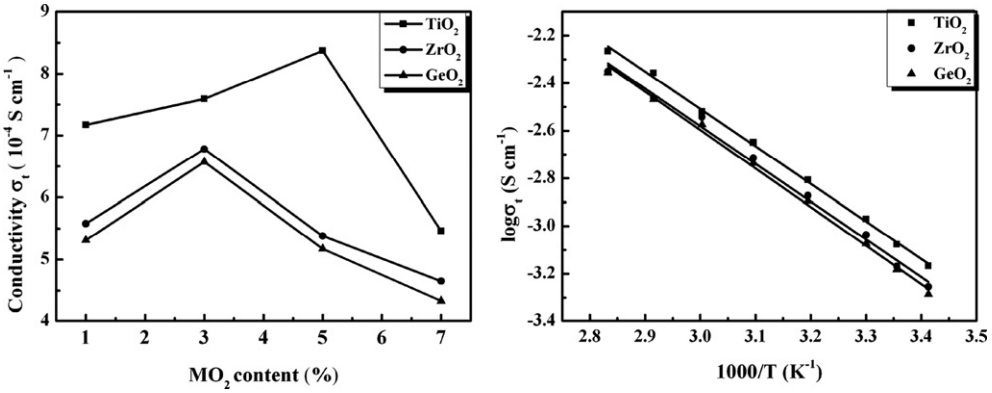

Fig. 3. Electrical conductivities of tape-cast (■) LAGP–TiO_2, (●) LAGP–ZrO_2, and (▲) LAGP–GeO_2 at 25 °C as a function of the content of MO_2 and the Arrhenius total electrical conductivity plots of tape-cast (■) LAGP–5 wt.% TiO_2, (●) LAGP–3 wt.% ZrO_2 and (▲) LAGP–3 wt.% GeO_2.

of the H-type cell after storage for 7 days. The impedance profiles of the LAGP–5 wt.% TiO_2–epoxy hybrid sheet are compared with that of the LAGP–5 wt.% TiO_2 sheet in Fig. 5. The bulk conductivity of the hybrid sheet is the same as that of the sheet without epoxy resin, but the grain boundary conductivity of the hybrid sheet is significantly decreased from 6.83×10^{-3} S cm^{-1} for the sheet without epoxy resin to 6.93×10^{-4} S cm^{-1}. The low grain boundary conductivity (high resistance) may be due to the presence of an insulator phase of epoxy resin at the grain boundary. The total electrical conductivity of the hybrid sheet (4.19×10^{-4} S cm^{-1}) at 25 °C is approximately half that of the LAGP–5 wt.% TiO_2 sheet without epoxy resin, and higher than that of the dense LATP glass ceramic supplied by Ohara Co., Japan (3.5×10^{-4} S cm^{-1}) [13] and comparable to that of an LATP–epoxy hybrid film [12]. The mechanical properties of the LAGP–5 wt.% TiO_2 were improved by the addition of epoxy resin, The three-point bending strength at room temperature of 74 N mm^{-2} for LAGP–5 wt.% TiO_2 was increased to 111 N mm^{-2} by the addition of epoxy resin, which is also comparable with that of the Ohara LATP glass ceramic plate and higher than that of the LATP–epoxy hybrid film (52 N mm^{-2}).

The water impermeable LAGP hybrid sheet should be stable in an aqueous solution saturated with LiOH, because the reaction product of aqueous lithium-air batteries is LiOH. We have previously reported that a saturated aqueous solution of LiCl and LiOH has a low pH of ca. 9, due to the low dissociation of LiOH in the presence of a high concentration of Li^+ [8]. The impedance profiles of the LAGP–5 wt.% TiO_2–epoxy resin hybrid sheet immersed in saturated LiCl aqueous solution and saturated LiCl and LiOH aqueous solution at 50 °C for one week are shown in Fig. 5. Both the bulk and grain boundary resistances are comparable before and after immersion in these solutions. XRD analysis also indicated no structural change in the hybrid sheets by immersion in these solutions. Therefore, it could be concluded that the LAGP–5 wt.% TiO_2–epoxy resin hybrid sheet is stable in saturated LiCl and LiOH aqueous solution and is thus suitable as the protective layer of a water-stable lithium metal electrode.

The stability and electrochemical performance of the water-stable lithium metal electrode with the LAGP–5 wt.% TiO_2–epoxy resin hybrid sheet as the protective layer were examined. Impedance profiles of the Li/PEO_{18}LiTFSI–10 wt.% $BaTiO_3$/LAGP–5 wt.% TiO_2–epoxy resin hybrid/saturated LiCl aqueous solution/Pt plate with Pt black, air cell measured at 60 °C are shown as a function of the storage time in Fig. 6. The polymer electrolyte was used to prevent direct contact between the lithium metal and the LAGP sheet, because LAGP is unstable in contact with lithium metal [9]. The room temperature conductivity of the polymer electrolyte was too low to pass a high current; therefore, the stability test was

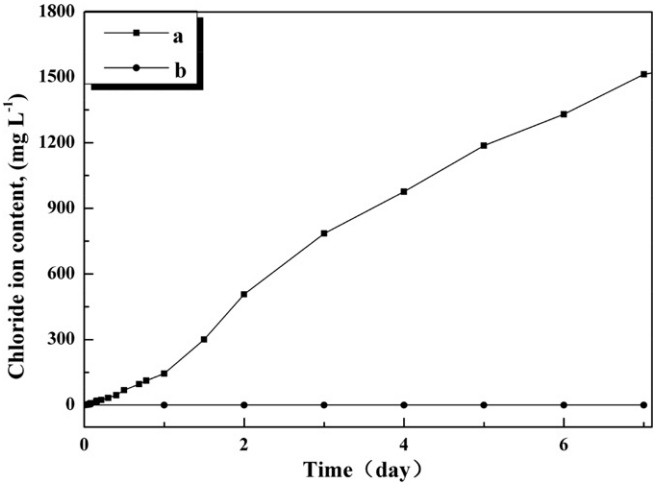

Fig. 4. The water permeation test results of tape-cast (a) LAGP–5 wt.% TiO_2 and (b) LAGP–5 wt.% TiO_2–epoxy resin hybrid sheets at room temperature.

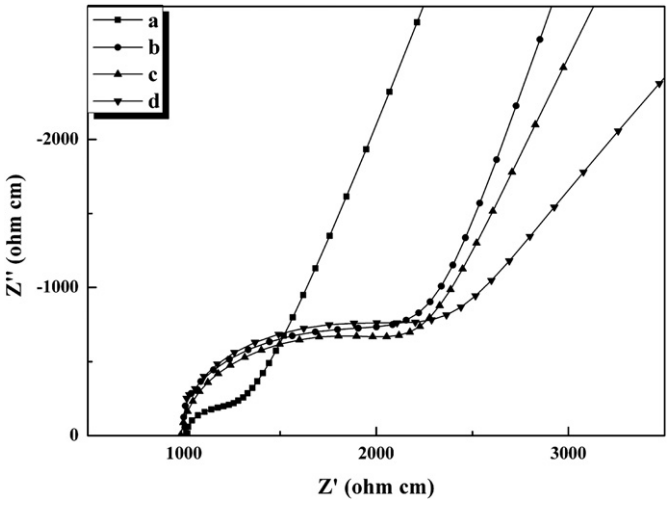

Fig. 5. Impedance profiles of tape-cast (a) LAGP–5 wt.% TiO_2, (b) LAGP–5 wt.% TiO_2–epoxy, and (c) LAGP–5 wt.% TiO_2–epoxy sheets immersed in saturated LiCl aqueous solution at 50 °C for one week, and (d) LAGP–5 wt.% TiO_2–epoxy resin hybrid sheet immersed in saturated LiCl and LiOH aqueous solution at 50 °C for one week.

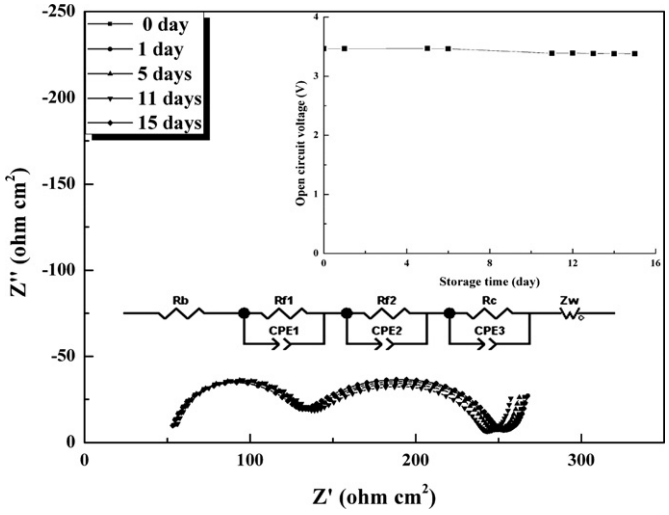

Fig. 6. Impedance profiles of the Li/PEO_{18}LiTFSI–10 wt.% $BaTiO_3$/LAGP–5 wt.% TiO_2–epoxy resin hybrid sheet/saturated LiCl aqueous solution/Pt plate with Pt black, air cell at 60 °C as a function of storage time and the change of OCV with time.

conducted at 60 °C. Two semicircles are evident in the impedance profiles. The semicircle at the high frequency range corresponds to the contribution of the grain boundary resistance of the LAGP hybrid film and polymer electrolyte (R_1), because similar semicircles were observed in the same frequency range for Au/LAGP–5 wt.% TiO_2–epoxy resin/Au and Au/PEO_{18}LiTFSI–10 wt.% $BaTiO_3$/Au. The semicircle in the low frequency range may be attributed to the interface layer between lithium and the polymer electrolyte (R_2) and the charge transfer resistance (R_c) between lithium metal and the interface layer [14]. No significant change of the impedance profiles was observed for a storage time of 15 days. If water penetrates through the film, it will react with lithium through the PEO layer (PEO is soluble in water), and the cell resistance would be significantly increased. However, the lack of change in the cell resistance confirms that the hybrid sheet is water impermeable, as observed in the water penetration test. The impedance spectra were analyzed using the equivalent circuit shown as an inset in Fig. 6, and the following results were obtained at 60 °C: $R_b = 50$, $R_1 = 83$, $R_2 = 98$, and $R_c = 17\ \Omega\ cm^2$, where R_b is the bulk resistance of the hybrid sheet and the polymer electrolyte. The charge transfer resistance is not as high as the other resistances. To reduce the cell resistance, the resistance of LAGP ($R_b + R_1$) and the interface layer between lithium and polymer electrolyte (R_2) should be improved. Recently, Liu et al. reported that the interface resistance between PEO_{18}LiTFSI and lithium was reduced to ca. 25 $\Omega\ cm^2$ by the co-doping of an ionic liquid and nanosize SiO_2 into the polymer electrolyte [15]. The change of the lithium electrode OCV with the storage time is shown as an inset in Fig. 6. The stable OCV for the lithium electrode of 3.4 V *vs.* Pt/air was observed for 15 days, and is comparable to theoretical OCV.

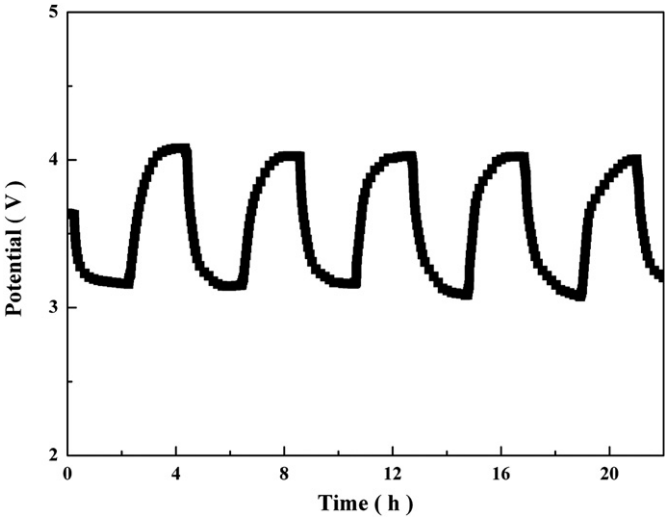

Fig. 7. Change of the lithium electrode potential at 0.5 mA cm^2 and 60 °C in the Li/PEO_{18}LiTFSI–10 wt.% $BaTiO_3$/LAGP–5 wt.% TiO_2–epoxy resin/saturated LiCl aqueous solution/Pt plate with Pt black, air cell.

Fig. 7 shows the change in the potential of the lithium electrode by lithium deposition and stripping for the Li/PEO_{18}LiTFSI–10 wt.% $BaTiO_3$/LAGP–5 wt.% TiO_2–epoxy resin/saturated LiCl aqueous solution/Pt plate with Pt black, air cell at 60 °C, where the lithium electrode potentials were measured using a Pt black reference electrode. The lithium deposition and stripping overpotential of the water-stable electrode was around 0.5 V at 0.5 mA cm^{-2}. The overpotential caused by cell resistance is 0.125 V; therefore, the electrode polarization by the lithium deposition and stripping processes should be reduced to pass a higher current density for application as a power source in electrical vehicles.

4. Conclusions

A high conductivity and water impermeable LAGP–5 wt.% TiO_2–epoxy hybrid sheet with a thickness of ca. 200 μm was prepared by the tape casting method. The electrical conductivity of the hybrid film was 4.19×10^{-4} S cm^{-1} at 25 °C, which is comparable to that of a tape-cast LATP–3 wt.% TiO_2–epoxy sheet and is higher than that of an Ohara LATP glass ceramic plate. The three-point bending strength of the LAGP–epoxy hybrid film was 111 N mm^{-2}, which is comparable to that of the Ohara glass ceramic, and higher than that of LATP–epoxy hybrid sheet at 60–100 N mm^{-2}. A water-stable lithium electrode with LAGP–5 wt.% TiO_2–epoxy resin hybrid protective film with high conductivity and excellent mechanical properties was successfully operated in saturated LiCl aqueous solution. Thus, the hybrid sheet is attractive as a protective layer for the water-stable lithium metal electrode of aqueous lithium-air rechargeable batteries.

References

[1] M. Armand, J.M. Tarascon, Nature 451 (2008) 652.
[2] G. Girishkumar, B. McCloskey, A.C. Luntz, S. Swanson, W. Wilcke, J. Phys. Chem. Lett. 1 (2010) 2193.
[3] A. Kraytsberg, Y. Ein-Eli, J. Power Sources 196 (2011) 886.
[4] J. Christensen, P. Albertus, R.S. Sanchez-Carrera, T. Lohmann, B. Kozinsky, R. Liedtke, J. Ahmed, A. Kojic, J. Electrochem. Soc. 159 (2012) R1.
[5] K.M. Abraham, Z. Jiang, J. Electrochem. Soc. 143 (1996) 1.
[6] T. Zhang, S. Liu, N. Imanishi, A. Hirano, Y. Takeda, O. Yamamoto, Electrochemistry 78 (2010) 360.
[7] S.J. Visco, E. Nimon, B. Latz, L.C.D. Jonghe, M.Y. Chu, Abstract #53, International Meeting on Lithium Batteries, Nara, Japan, 2004.
[8] Y. Shimonishi, T. Zhang, N. Imanishi, D. Im, D.J. Lee, A. Hirano, Y. Takeda, O. Yamamoto, N. Sammes, J. Power Sources 196 (2011) 5128.
[9] M. Zhang, K. Takahashi, N. Imanishi, Y. Takeda, O. Yamamoto, J. Electrochem. Soc. 159 (2012) A1114.
[10] S. Liu, N. Imanishi, T. Zhang, A. Hirano, Y. Takeda, O. Yamamoto, J. Yang, J. Power Sources 195 (2010) 6847.
[11] P.G. Bruce, A.R. West, J. Electrochem. Soc. 130 (1983) 662.
[12] K. Takahashi, P. Johnson, N. Imanishi, N. Sammes, Y. Takeda, O. Yamamoto, J. Electrochem. Soc. 159 (2012) A1065.
[13] K. Takahashi, J. Ohmuram, D. Im, D.J. Lee, T. Zhang, N. Imanishi, A. Hirano, M.B. Phillipps, Y. Takeda, O. Yamamoto, J. Electrochem. Soc. 159 (2012) A342.
[14] T. Zhang, N. Imanishi, S. Hasegawa, A. Hirano, J. Xie, Y. Takeda, O. Yamamoto, N. Sammes, Electrochem. Solid-State Lett. 12 (2009) A132.
[15] S. Liu, H. Wang, N. Imanishi, T. Zhang, A. Hirano, Y. Takeda, O. Yamamoto, J. Yang, J. Power Sources 196 (2011) 7681.